Proceedings of the 12th International Conference on Fluid Flow, Heat and Mass Transfer (FFHMT 2025)
July 15, 2025 - July 17, 2025 | Imperial College London Conference, London, United Kingdom
Paper No. 236
DOI: 10.11159/ffhmt25.236

Experimental Study of Axial Fan Performances Operating In Constrained Environment: Application of Axial and Combined Axial–Radial Blockage

A. Larabi[1], A. Mammeri[2,3], T. Azzam[1], M. Pereira[2], F. Ravelet[2], M. Mekadem[1], H. Oualli[1] and F. Bakir[2,*]
[1]Ecole Militaire Polytechnique, Laboratoire de Mécanique des Fluides,
BP17 Bordj El Bahri, 16046 Algiers, ALGERIA
abderrahim.larabi@emp.mdn.dz; tarek.azzam@emp.mdn.dz; mahmoud.mekadem@emp.mdn.dz; hamid.oualli@emp.mdn.dz
[2]Arts et Métiers Institute of Technology, CNAM, LIFSE, HESAM University,
151 Boulevard de l'Hôpital, F-75013 Paris, France
michael.pereira@ensam.eu; florent.ravelet@ensam.eu; farid.bakir@ensam.eu
[3]Valeo Thermal Systems, La Verriere, 78320, Paris, France
amrid.mammeri@valeo.com
*Corresponding author(s). E-mail(s): *Farid.Bakir@ensam.eu*

***Abstract* -** This paper aimed to develop an experimental procedure for axial fans characterisation operating in constrained fields. The influence of an obstacle located downstream of a fan is studied experimentally on standardised test bench of the suction box type under different specific angular speeds. The axial fan of forward sweep category operates in free field referred as baseline configuration and in fields constrained by two blocking configurations axial and combined axial-radial. The blockages are produced by a flat plate, perpendicular to the axis of rotation of the fan for axial blockage case and two other plates placed radially for combined axial-radial blockage case, modelling, for example, the obstruction of a car internal combustion engine block. The four sets of global performances (pressure rise, flow rate, mechanical power and static efficiency) evolving with the different obstacles are compared to highlight their similarities. Variations in pressure rise as a function of flow rate were observed as the obstacle was changed depending upon the operating regime of the fan weather is working on axial or radial pattern discharge. The characteristic curves seem to evolve with substantial gain compared to the free field case especially when the blockage matched the flow configuration in the fans' wake.

***Keywords*:** axial fans, downstream blocking conditions, performance, axial and radial flow patterns

1. Introduction

Axial fans are recognized for their ability to move a large amount of air at low pressure, and they are frequently utilized in various settings such as ventilation, cooling, and heating systems. To ensure that they cover a wide range of operating conditions and provide acoustic comfort, efforts are made to enhance their aerodynamic performances and minimize their sound emission during operation. The use of flow control techniques can improve the performance of fans by minimizing issues associated with the airflow over its blades, hub, and shroud ring. In this regard, passive air injection is a highly effective approach due to its applicability and efficiency. Within this framework, enhancing these fans' efficiency in terms of the power they provide and the airflow they generate is one of the main research goals. Reducing noise in these cooling systems is also becoming more and more important. in keeping with the main objective of enhancing aerodynamic performance. This focus on noise reduction is particularly relevant in light of the growing popularity of electric vehicles among automakers, demonstrating a shared dedication to improving human comfort in tandem with technology improvements. It is also consistent with more general commitments to adhere to stringent environmental standards.

The improvement of aerodynamic performance, especially through flow control techniques, has been the subject of several earlier studies. Studies by Azzam et al. [1], Pereira et al. [2], and Bouanik et al. [3] are noteworthy contributions that examine the efficacy of active control strategies both experimentally and numerically. Together with additional axial turbomachinery topologies examined by Neuhaus and Neise [4], Sheng and Zhao [5], and Chen et al. [6], these works particularly look at the same hollow fan geometry covered in the current analysis. Although active control techniques have the potential to improve performance, they are frequently expensive and logistically difficult, especially when it comes to managing space in rotating systems. Researchers are urged to investigate passive control systems as an alternative. Works by Nadeau [7], Buisson et al. [8], S. Chen et al. [9], and L. Chen et al. [10] that concentrate on geometrical modifications as a control strategy, as well as passive injection strategies examined by Eberlinc et al. [11] and Wasilczuk et al. [12], are noteworthy contributions in this area.

However, these methods do not consider the fan environment as many of such fans; which are generally used in cooling systems; discharge onto obstacles in their immediate wake. In cars, the air enters through the front grille. The air drawn in by the fan passes through the heat exchanger. The compactness and design of modern vehicles means that the combustion engine is placed in the immediate vicinity of the fan. The problem is similar for computers, where the processor fan generally blows over a heat sink. The presence of the obstacle, perpendicular to the axial direction, causes the flow to bend sharply towards the radial direction. These fans are said to work in constrained fields.

In the accessible literature, there are still few studies dealing with the effect of downstream blocking. Gifford et al. [13] studied two fans coupled to an automotive cooling system. It highlights the fact that an obstacle such as a plate, placed perpendicular to the axis of rotation, causes a drop in the pressure rise when the fan is running. The drop is more noticeable on the low-pressure fan than on the high-pressure fan. The authors supplement the study of global characteristics with LDV measurements of the wake. They emphasise the importance of the radial component in the case of blocking. Vad and Bencze [14] use LDV to measure the radial velocity profiles behind several fans and give certain design rules relating to this component.

In this work, an axial forward sweep blade fan designed for the automotive cooling industry is studied with a view to taking into account the effect of blockage at the design stage as it meant principally to work in constrained field. The aim is to highlight similarities in the evolution of its aeraulic performance as a function of the severity of different blockage scenarios. The study has resulted in significant improvements in aerodynamic performance. It has the potential to expand the application of axial fans to confined spaces, including those affected by downstream blocking effects caused by system components installed near the fan exit taking advantage of flow topology in the fan' wake.

2. Experimental Setup

2.1. Fan geometry

In the automotive sector, axial fans are mainly used to reinforce the flow of air through the finned grid of the cooling radiator. Forced convection heat exchange ensures cooling as the vehicle moves away from the speed threshold. The fan is fitted with an electric motor that is activated when the natural air flow is no longer sufficient to lower the temperature of the coolant in the radiator. It is installed in the fan motor assembly (GMV).

Fig. 1: Axial fan geometry -type forward sweep.

The aim here is to study a car cooling fan illustrated in Fig. 1 and whose characteristics are given in Table 1. It is fitted with a DC motor which is mounted and fixed in a cylindrical casing. Today's high-tech industries need cooling products that consume little energy and reduce high heat generation. DC axial fans are designed for applications that require high-performance cooling and protection against harsh weather conditions in outdoor and extreme environments, offering much higher efficiency in comparison to fans with asynchronous motors. To vary the rotation speed of the fan, a power supply equipped with a potentiometer is used, delivering a maximum voltage of $12V$ with a current of $10A$, thus achieving a speed of rotation of around $1700\ rpm$.

Table 1: Axial Fan main characteristics.

Designation	Value	Designation	Value
Rated Capacity [W]	250	Support arms	3
Outer Diameter [mm]	350	Weight [kg]	2.26
Number of Blades	7	Operation Mode	Electrical DC

2.2. Testing bench and measurement system

Fig.2 depicts the experimental set-up used to determine the overall aeraulic characteristics of axial fan in open configuration. The suction box was designed and manufactured in a cooperation between the LMF laboratory at Ecole Militaire Polytechnique and the LIFSE laboratory at Arts et Métiers ParisTech according to the ISO-5801 standards. It forms a cube measuring $1.3 \times 1.3 \times 1.8\,m$. The DC motor drives the fan and a power supply control system ensures that the speed of rotation ω remains constant at ±0.2%. The flow rate is set and measured in accordance with ISO-5801 standard by adjusting the bench's air impedance using calibrated diaphragms of various diameters that are put on the opposite side of the rectangular box. A perforated plate inside the box limits the pre-rotation of the fluid that could be induced by the fan. The large plate simulates the axial blocking of a motor block whereas the horizontal small plates simulate the combined axial-radial blockage. The distances L are measured between the rear of the fan and the obstacle plate where the distances R are taken from the fan centre to the desired position. Blocking conditions values L/D are 0.22 and 0.36. The pressure rise ΔP is measured to an absolute accuracy of ±0.1Pa. The mechanical power absorbed by the fan, aeraulic power and fan efficiency are estimated by using the method of separated loses. The accuracy of the complete system leads to a static efficiency accuracy of ±0.5%. The measurements were repeated 4 times and repeatability is the main source of uncertainty.

Initially, in order to investigate the behaviour of the fan over a wide range of operating flow conditions, eight diaphragm diameters are tested. The diameters of the diaphragms are reported in Table 2. Then for a given angular rotation speed the values for both the inductor terminal voltage of the DC motor, the corresponding current in the field circuit and the pressure difference generated by the fan ΔP were taken.

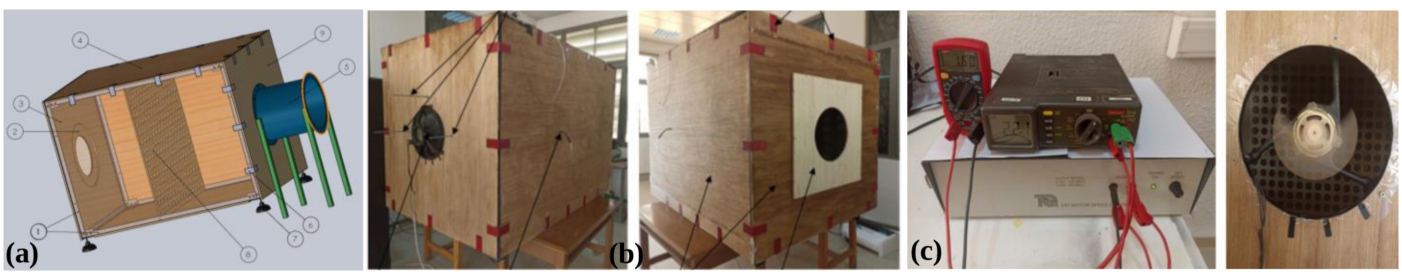

Fig. 2: **(a)** Cut of the experimental test bench, **(b)** *ISO* - 5801 test bench with Axial fan motor assembly, **(c)** Wiring diagram for the fan installation.

Table 2: Diaphragm's diameters tested.

φ[mm]	77	151	190	138	267	300	336	375

2.3. Separated losses method

The electrical diagram shown in Fig. 2 (b) and (c) consists of DC motor, fan and generator (variable frequency drive + power supply). The assembly involves a voltmeter connected in parallel with the generator and an amperemeter connected in series with respect to the generator and the fan. In order to evaluate the electrical, mechanical and aeraulic power, first the internal resistance R_i generated by the motor coil is measured under circumstances where the rotor is blocked using a multi-meter and found to be $0.26\,\Omega$. Then followed by another test with motor no-load in order to determine constant losses, torque and efficiency.

The expressions used for the calculations are as follows and in accordance with *ISO-5801* standard [2]. The fan flow rate can be determined using this normative approach ensuring an accurate and reproducible assessment of the flow characteristics, based on established aerodynamic principles.

$$Q_v = \alpha \times A \times \sqrt{\left(\frac{2 \times \Delta \mathrm{P}}{\rho_{air}}\right)} = 0{,}6 \times \left(\frac{\pi D^2}{4}\right) \times \sqrt{\left(\frac{2 \times \Delta \mathrm{P}}{1{,}21}\right)} \tag{1}$$

Such that, α is the flow rate coefficient equal to 0.6 and A is the diaphragm orifice cross-section.
The aeraulic power of the circuit is calculated as follow:

$$P_{aeraulic} = \Delta \mathrm{P}_{\mathrm{stat}} \times Q_v \tag{2}$$

Mechanical power is obtained using the classic method of separate losses, as like:

$$P_{mechanical} = (U \times I) - (R_i \times I^2) - (U_0 \times I_0 - R_i \times I_0^2) \tag{3}$$

Where, U_0 is the no-load rotor terminal voltage at a given rotation speed, I_0 is the no-load rotor terminal current at the same rotation speed and R_i is the rotor internal resistance measured earlier.
It can be seen that mechanical power is made up of three factors: $(U \times I)$ is the electrical power, $(R_i \times I^2)$ is Joule effect losses and $(U_0 \times I_0 - R_i \times I_0^2)$ characterises the no-load losses.

The last but not the least, the aeraulic efficiency can be written as follow:

$$\eta_{aeraulic} = \frac{P_{aeraulic}}{P_{mechanical}} = \frac{\Delta \mathrm{P}_{\mathrm{stat}} \times Q_v}{(U \times I) - (R_i \times I^2) - (U_0 \times I_0 - R_i \times I_0^2)} \tag{4}$$

Finally, the overall performance of the four fans is presented in dimensionless values such that the usual flow coefficient Φ and pressure coefficient Ψ parameters are given in the following expressions.

$$\Phi = \frac{Q_v}{\pi\omega \times R_{out}^3} \tag{5}$$

$$\Psi = \frac{\Delta \mathrm{P}}{\rho\omega^2 \times R_{out}^2} \tag{6}$$

2.4. Blockage design

Low-pressure fans (LPF) are particularly well suited to the needs of modern cooling systems, as they have relatively stable performance curves, unlike high-pressure fans (HPF). In order to design an LPF capable of meeting the specific constraints of new thermal engines, it is essential to have an in-depth understanding of the influence of the surrounding components - particularly those present under the bonnet - on the fan's performance. With this in mind, the study focused on the effect of downstream blockage caused by the presence of the engine block. To simulate this phenomenon in a simplified way, a flat plate was used as an obstacle model. The influence of this obstacle was studied experimentally for different angular speeds of rotation of the fan, using a standardised test bench of the suction box type, allowing precise evaluation of performance under controlled conditions.

The aim of this study is to experimentally quantify the interaction between a fan and the engine block, in order to determine the optimum position between these two components. To this end, a series of additional experiments were carried out to analyse the relationship between fan performance and the distance separating the fan from the motor block. After characterising the fan without the blocking effect, the blocking plates were mounted. This is clearly illustrated in Fig.3, which shows the two blocking configurations adopted, i.e. ‘Axial blocking’ and ‘combined Axial–Radial blocking’.

Fig. 3: Axial blockage (first left) and combined Axial–Radial blockage configurations (right images).

The blocking device is made of a flat plate of plywood measuring $1000 \times 1000 \times 15\ mm$, placed perpendicular to the axis of rotation of the rotor. The axial distance, L between the fan and the plate is measured from the trailing edge of the blades to the surface of the plate. To ensure precise adjustment of this distance, the plate is fixed using four identical threaded rods (length $300mm$), mounted on the discharge side of the casing and arranged symmetrically around the fan axis. Each rod is marked with two predefined positions, allowing two different axial locking configurations to be achieved: $75mm$ and $125mm$.

In addition, the plate has four longitudinal grooves that allow radial adjustment of its position in relation to the fan axis. This makes it possible to study the effect of the lateral offset (or in our case radial blocking) of the obstacle on the aerodynamic performance of the fan. In relation to the centre of the fan, the first groove is placed at $225mm$ and then the others in $50mm$ increments. For each blocking configuration, the tests are carried out for eight different diaphragm diameters (see Table.2) and three fan speeds: 700, 1100 and $1500\ rpm$.

3. Results

3.1. Baseline configuration – Fan in free field flow

Fig.4 depicts the results obtained for the fan characteristics at rotation speeds of 700 rpm, 1100 rpm and 1500 rpm. The trend in the evolution of the obtained curves and the increasing effect of the speed of rotation on the fan characteristic are in line with the literature. The second point of the characteristic corresponding to the 151mm diaphragm diameter shows a slight decrease in the torque (pressure-flow). This may be related to the forward sweep shape of the blades which deserves to be well studied in future work (numerical and experimental), while trying to identify the local aerodynamic loss mechanism in the fan characteristic. Furthermore, to demonstrate the complexity of analysing the characteristics of the axial fan, taking a case with a rotation speed of 1100 rpm, according to the test carried out we verified that although the fan is on axial configuration (geometrically), it changes its discharge mode (downstream flow) according to the flow coefficient. Two discharge modes are found at both ends of the characteristic. The study of Periera et al. [2], having worked on a similar fan with forward sweep blades, numerically demonstrated the three-dimensional flow topology for these two ends of each corresponding curve (Fig. 4 – left and right streamlines).

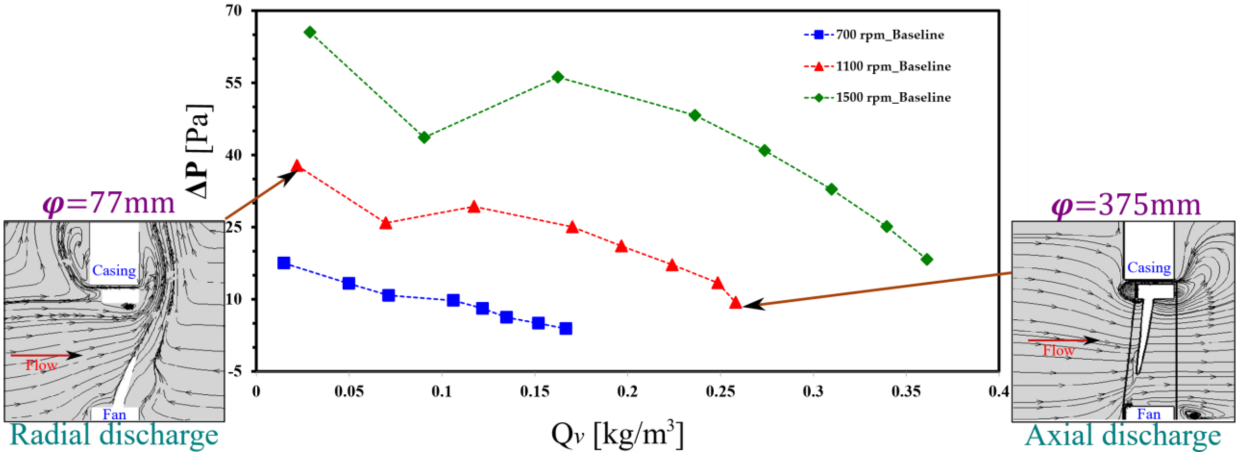

Fig. 4: Fan characteristics at baseline case at tested speeds.

On the one hand, a 'radial' flow topology at the fan outlet generated by the effect of the blades sweeping configuration (forward) and also the depression in the wake leads to a mass flow of the ambient air from the downstream infinite towards the fan then a reconduction under the centrifugal effect of the blades in the radial direction. On the other hand, an 'axial' flow topology where the effect of blade sweeping and centrifugal forces are neglected compared with the axial inertia of the suction. This leads to an axial flow in the fan's wake, which also sucks in ambient air on either side of the fan's axial discharge duct.

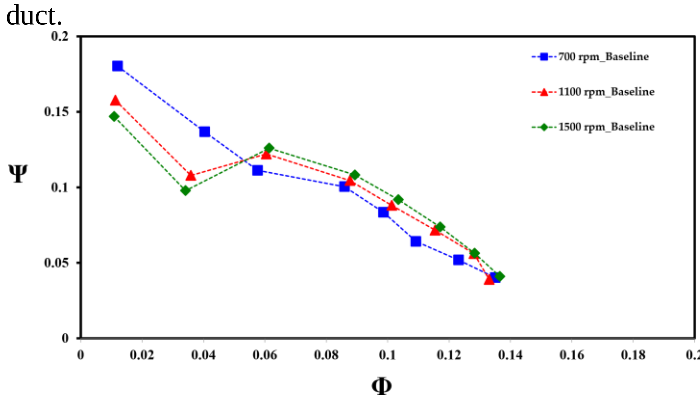

Fig. 5: Dimensionless fan characteristics at baseline case at tested speeds.

Fig.5 illustrates the evolution of the dimensionless parameters relating to the pressure-flow curve given respectively by the two coefficients of pressure (Ψ) and flow (Φ). The important thing to remember about this dimensionless transformation is to see the validity of the similarity principle. In fact, the similarity procedure makes it possible to extrapolate the results to other similar shapes, from small to large, while having the same dimensional curve and different operating conditions. From the results shown in the Fig. 5, it can be clearly seen that from the speed of 1100 rpm there is a convergence or, in other words, a superposition of the characteristics obtained at different speeds of rotation. Whereas, it can be seen that the speed 300 rpm does not converge well, due to phenomena of low Reynold's numbers (low speed of rotation). The 700 rpm speed tends to converge but shows some errors much more towards the first two points of the low flow rate characteristic.

3.2. Blocking configuration assessment – Fan under constrained flow field

The following table (Table 4) summarises the configurations processed in analysing the blockage effects on fan performances:

Table 4: Analysed Scenarios for blockage analysis.

Case#01	A single blocking plate positioned axially at 75*mm*.
Case#02	Case#01 and two additional 75*mm* wide radial plates inserted in the two grooves in the first position on either side of the fan axis.
Case#03	A single Blocking plate placed axially at 125*mm*.
Case#04	Case#03 and two additional 125*mm* wide radial plates inserted in the two grooves in the second position on either side of the fan axis.

- **Case#01 and #02 – Rotation speed 1500rpm**

Fig.6 shows the results obtained for a rotation speed of 1500 rpm with a blockage of 75*mm*, comparing three configurations: Baseline, Axial_75*mm* and Axial-Radial_75*mm* configurations. The plots demonstrate that blocking is an effective means of control for pressure-flow coefficients in accordance to blocking alone at 75*mm*. The situation is reversed for high flow coefficients, where combined blocking is more favourable than blocking alone. It would therefore be desirable in future work to use numerical modelling and, where possible, advanced experimental investigation to analyse the flow structures and provide possible explanations for the improvements observed (PIV or LDA analysis). Moreover, in case of such high rotation speed, and in comparison, with the speed of 1100 rpm, the following points can be noted: The performance improvement trend is almost identical. Also, for the high flow rate coefficients (operating range relative to the last four points), no significant improvement in the dimensionless curve (pressure-flow rate), which has repercussions on the simultaneous evolution of aeraulic power and efficiency in this operating range. Thus, the stability of the mechanical power is significant 28*W* for 1500 rpm (Fig. 6 (d)) compared with 11*W* for lower rotation speeds. This is due to the friction and viscous effects generated on the fan at high speeds, which in some cases weakens the efficiency. Finally, the efficiency curve (η) (Fig. 6 (c)) is the most revealing: Axial_75*mm* reaches a peak of almost 50%, much higher than in the baseline case. Although Axial – Radial_75*mm* has a slightly lower efficiency, it is still better than the baseline configuration.

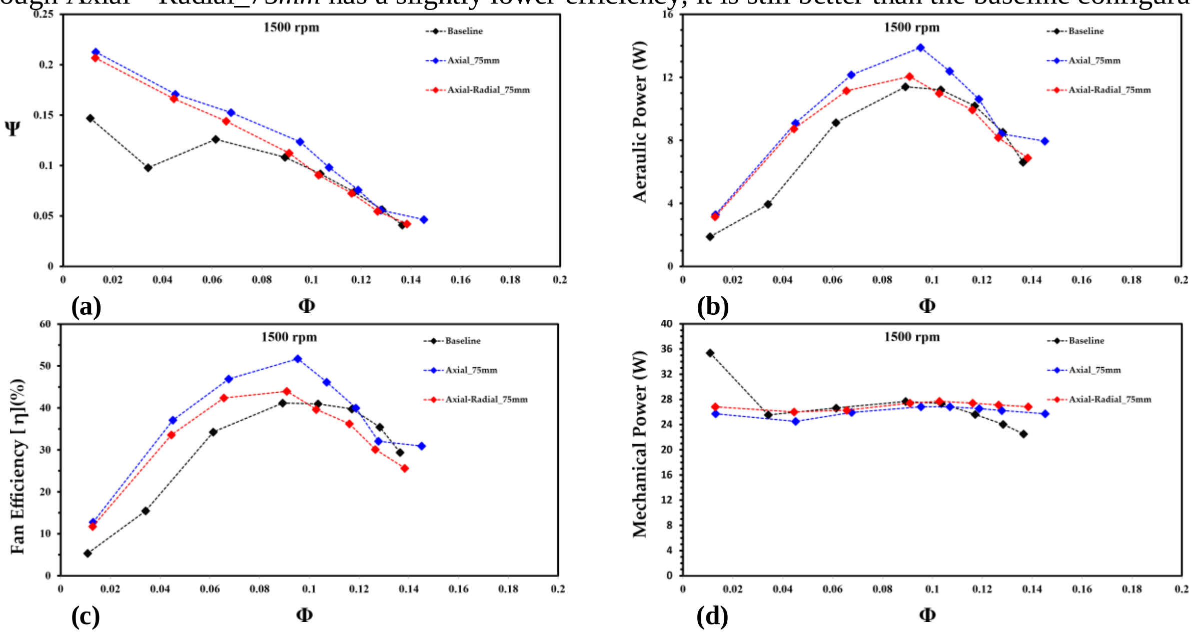

Fig. 6: Overall fan aerodynamic performances for baseline for Axial and Axial-Radial-75mm scenarios – Angular speed of 1500 rpm, **(a)** Dimensionless characteristics, **(b)** Aeraulic power, **(c)** Fan efficiency and **(d)** Mechanical power.

- **Case#03 and 04 – Rotation speed 1500rpm**

At 1500 rpm, improvements can still be seen in the dimensionless characteristic and also in the aeraulic power. However, in the graph (Fig.7 (d)) for the mechanical power is stabilised at slightly high values due to the effects of friction at very high speeds. Compared with the rotation speed of 1100 rpm, the improvement in maximum efficiency decreases to around 60%.

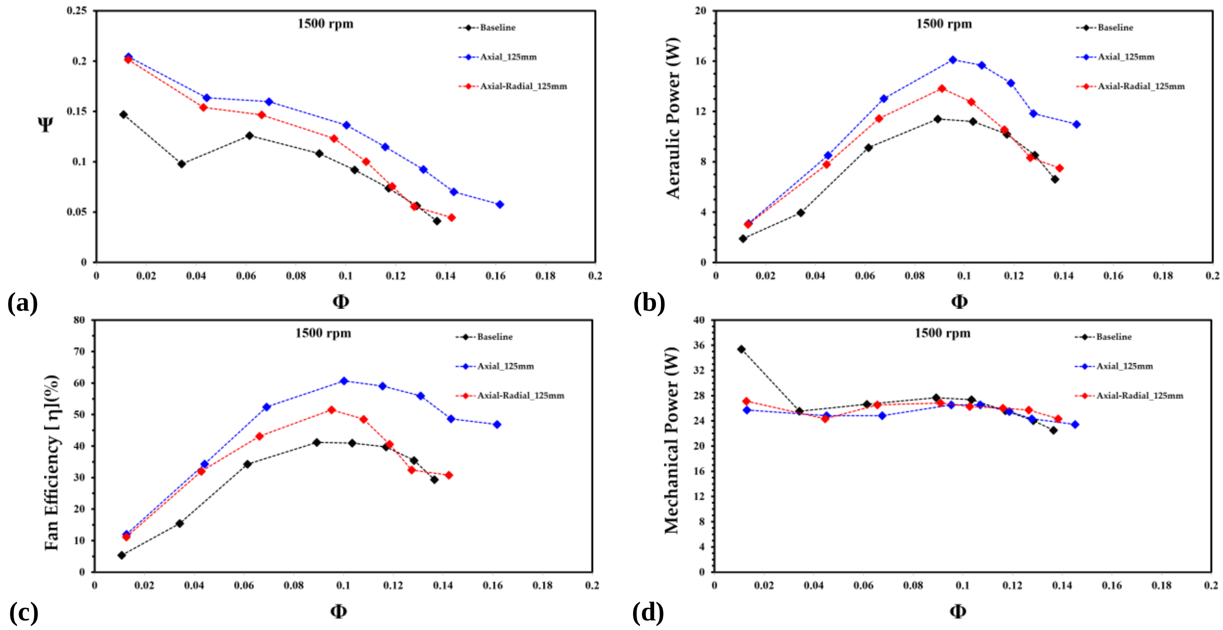

Fig. 7: Overall fan aerodynamic performances for baseline for Axial and Axial-Radial-125mm scenarios – Angular speed of 1500 rpm, **(a)** Dimensionless characteristics, **(b)** Aeraulic power, **(c)** Fan efficiency and **(d)** Mechanical power.

It should be noted that, for the 125*mm* axial blockage alone, the aeraulic power plot (Fig.6 (b)) quoted for the 1500 rpm speed and for the high flow coefficients (05 last point) is better spread out than for the 1500 rpm speed alone, this is due to the significant improvement in this operating range observed for the dimensionless curves.

4. Conclusion

In this work, an aeraulic study on a standardised test bench of an axial cooling fan for a land vehicle is presented. The aim is to set up an experimental procedure for studying the operation of this fan in free and constrained field. For such scenarios, we opted for geometric configurations of the fan blocking in the downstream side. Four blocking configurations were tested; two vertical plates placed axially downstream at 75*mm* and 125*mm* and two others combining the first two with another blocking in the radial discharge direction of the fan. The radial blocking is insured by two plates positioned horizontally (vertical to the axial plate) and symmetrically in relation to the fan axis. Depending on the different operating conditions (diaphragm diameter, speed of rotation, etc.) and the geometry of the blocking (Axial and Axial–Radial position), the experimental measurements carried out enabled us to characterise the operation of the fan through the pressure-flow curves, aeraulic power, mechanical power and fan efficiency for the two configurations, baseline and blocking cases. Thus, the results show unexpected improvements when the blocking is applied for some fan operating situations. Axial blocking alone is more cost-effective than the combined Axial-Radial configuration. In general, better performance was also achieved for the axial position of the 125*mm* blockage. To sum up, we can say that certain downstream fan blocking configurations can help to improve its operation in practice. We still need to deep investigate the sources of aerodynamic losses for controlling the effective flow, using advanced instrumentation and detailed numerical studies of the flow structure upstream and downstream of the fan.

References

[1] Azzam, T., Paridaens, R., Ravelet, F., Khelladi, S., Oualli, H., & Bakir, F. (2017). Experimental investigation of an actively controlled automotive cooling fan using steady air injection in the leakage gap. *Proceedings of the Institution*

of Mechanical Engineers, Part A: Journal of Power and Energy, 231(1), 59–67. DOI: *https://doi.org/10.1177/0957650916688120*.

[2] Pereira, M., Ravelet, F., Azzouz, K., Azzam, T., Oualli, H., Kouidri, S., & Bakir, F. (2021). Improved aerodynamics of a hollow-blade axial flow fan by controlling the leakage flow rate by air injection at the rotating shroud. *Entropy*, *23*(7). DOI: *https://doi.org/10.3390/e23070877*.

[3] Bouanik, A., Azzam, T., Abbasnezhad, N., Larabi, A., Mekadem, M., & Bakir, F. (2024). Active air injection control to enhance performance of hollowbladed axial fan: a numerical study. *Journal of Applied Fluid Mechanics*, 17(3), 519–533. DOI: *https://doi.org/10.47176/jafm.17.3.2201*.

[4] Neuhaus, L., & Neise, W. (2007). Active control to improve the aerodynamic performance and reduce the tip clearance noise of axial turbomachines with steady air injection into the tip clearance gap. *In R. King (Ed.), Active Flow Control*, pp. 293–306. Springer Berlin Heidelberg. DOI: *https://doi.org/10.1007/978-3-540-71439-2_18*.

[5] Chen, S., Zhou, Z., Meng, Q., Wang, S., & Zhou, X. (2017). Experiment study of the winglet-cavity tip on the aerodynamic performance in a turbine cascade. *Proceedings of the Institution of Mechanical Engineers, Part A: Journal of Power and Energy*, 231(7), 676–685. DOI: *https://doi.org/10.1177/0957650917720560*.

[6] Chen, S., Gong, Y., & Zeng, C. (2022). Experimental investigation of hole-type bleed for active flow control in an axial compressor cascade with tip clearance. *Aerospace Science and Technology*, 128, 107790. DOI: *https://doi.org/10.1016/j.ast.2022.107790*.

[7] Nadeau, S. (2005). *Integral tip seal in a fan-shroud structure*. Siemens VDO Automotive Inc., US Patent 56874990.

[8] Buisson, M., Ferrand, P., Soulat, L., Aubert, S., Moreau, S., Rambeau, C., & Henner, M. (2013). Optimal design of an automotive fan using the Turb'Opty meta-model. *Computers and Fluids*, 80(1), 207–213. DOI:*https://doi.org/10.1016/j.compfluid.2012.03.015*.

[9] Chen, S., Zhou, Z., Meng, Q., Wang, S., & Zhou, X. (2017). Experiment study of the winglet-cavity tip on the aerodynamic performance in a turbine cascade. *Proceedings of the Institution of Mechanical Engineers, Part A: Journal of Power and Energy*, 231(7), 676–685. DOI: https://doi.org/10.1177/0957650917720560.

[10] Chen, L., Xie, H., Xu, J., Dai, R., & Chen, J. (2018). Experimental and numerical study on the performance of an axial fan with a Gurney flap. *Advances in Mechanical Engineering*, *10*(10), 1–17. DOI: *https://doi.org/10.1177/1687814018803804*.

[11] Eberlinc, M., Širok, B., Dular, M., & Hočevar, M. (2009). Modification of axial fan flow by trailing edge self-induced blowing. *Journal of Fluids Engineering*, 131(11). DOI: *https://doi.org/10.1115/1.4000345*.

[12] Wasilczuk, F., Flaszynski, P., Kaczynski, P., Szwaba, R., Doerffer, P., & Marugi, K. (2021). Air curtain application for leakage reduction in gas turbine shroud sealing. *Aerospace Science and Technology*, *112*, 106636. DOI: *https://doi.org/10.1016/j.ast.2021.106636*.

[13] N. L. Gifford, E. Savory, and R. J. Martinuzzi, (2007). Experimental Study of Automotive Cooling Fan Aerodynamics. *SAE Paper* No. 2007-01-1525. DOI: *https://doi.org/10.4271/2007-01-1525*.

[14] J. Vad, F. Bencze (1998). Three-dimensional flow in axial flow fans of non-free vortex design. *International Journal of Heat and Fluid Flow*, 19(1998), 601-607. DOI: *https://doi.org/10.1016/S0142-727X(98)10004-8*.